HHS Public Access

Author manuscript

Neuroscience. Author manuscript; available in PMC 2021 November 21.

Published in final edited form as:

Neuroscience. 2020 November 21; 449: 63–73. doi:10.1016/j.neuroscience.2020.09.056.

Spatiotemporal contrast sensitivity of Brown-Norway rats under scotopic and photopic illumination

Nicholas P. Johnson[1], **Sarah M. Gregorich**[2], **Christopher L. Passaglia**[1,2,3]

[1]University of South Florida, Molecular Pharmacology & Physiology Department, 12901 Bruce B Downs Blvd MDC 40, Tampa, FL 33612

[2]University of South Florida, Medical Engineering Department, 4202 E Fowler Ave, Tampa, FL 33620

[3]University of South Florida, Ophthalmology Department, 12901 Bruce B Downs Blvd MDC21, Tampa, FL 33612

Abstract

Rats are a popular animal model for vision research and for investigating disorders of the visual system. The study aimed to quantify the spatiotemporal contrast sensitivity function (CSF) of healthy adult Brown-Norway rats under scotopic and photopic illumination. Animals were trained to jump onto the one of two adjacent platforms behind which was displayed a sinewave grating pattern. Contrast thresholds of light- and dark-adapted rats were determined using a staircase method of adjustment for gratings that varied in spatial frequency (sf) and temporal frequency (tf) and ranged several log-units in mean luminance. Photopic CSFs showed strong bandpass spatial tuning, consistent with prior measurements, and weak bandpass temporal tuning. CSFs were parameterized by a truncated log-parabola model, yielding a peak contrast sensitivity of 52 ± 9, peak sf of 0.17 ± 0.05 cycles/degree, sf limit of 1.6 ± 0.3 cycles/degree, low sf attenuation of 85 ± 9%, peak tf of 1.7 ± 1.1 Hz, extrapolated tf limit of 166 ± 44 Hz, and low tf attenuation of 55 ± 12%. CSFs became more lowpass and decreased systematically in contrast sensitivity and spatiotemporal acuity as mean luminance was reduced. CSFs were also measured via the visual head-tracking reflex. Photopic contrast sensitivity, spatial acuity, and temporal acuity were all markedly below that of the grating detection task and optomotor findings for other rat strains. The CSF data provide a comprehensive and quantitative description of rat spatial and temporal vision and a benchmark for evaluating effects of ocular diseases on their ability to see.

Keywords

spatial acuity; temporal acuity; contrast threshold; frequency response; optomotor reflex

Corresponding author: Dr. Christopher L. Passaglia, Department of Medical Engineering, University of South Florida, 4202 E Fowler Ave, Tampa, FL 33620. Phone: 813-974-7140, passaglia@usf.edu.

Declarations of interest: none

Introduction

Researchers employ a variety of animal models to investigate the neural basis of visual behavior and disorders of the visual system. The choice of model is driven by a combination of factors, including size, accessibility, cost, and experimental method. Although primate models have the greatest translational relevance, rodent models can provide technical advantages that make them a popular subject of study. It may be debated whether rodents are a suitable model for human vision since they have relatively poor eyesight and a tiny visual cortex that performs multiple sensory functions [1]. Nevertheless, modern scientific advances in genetic engineering, electrophysiological recording, optical imaging, and disease induction techniques have led to an explosion of research on mouse and rat visual systems in the past two decades [2]. The work has revealed that rats are excellent for visual psychophysics as the animals can learn to perform many complex discrimination tasks [3–5] and even steer a motorized car [6]. Mice can also learn complex visual tasks [7–10] but generally take longer to train, perform less reliably, and cannot master some of the same tasks [8, 11–14].

Numerous vision tests have been developed to evaluate what and how well rodents can see [15]. The first was the jump test, in which animals discriminate high-contrast patterns by jumping from a small elevated stand through one of two adjacent doors [16]. Others are the poke and press tests, in which animal discriminate between a visual target and equiluminant non-targets by poking their nose through a hole or by pressing a lever or touchscreen [17–21]. Considerable training time is required for rodents to learn these tasks so the water test was introduced, which forces animals to find a submerged platform in one arm of a Y-shaped water tank [12, 13, 22]. Rats quickly associate a visual target with platform location in order to find rest, but the location of target detection is unknown since the animal is swimming around. The visual target in these tests has traditionally been a grating pattern displayed on an oscilloscope or computer monitor, enabling detailed measurement of rat contrast sensitivity and acuity [12, 17–19, 22, 23]. Abstract shapes and scenes have also been employed that show rodents can perform fairly advanced visual computations such as invariant object recognition, perceptual grouping, and collinear feature discrimination [20, 24–27]. Tests that do not require operant conditioning are generally employed to evaluate rodent vision in disease models. The most popular is the optomotor test, which bypasses the need for behavioral training by evoking eye- and head-tracking movements with widefield cylindrically-rotating patterns [28, 29]. The visual reflexes are driven by subcortical circuits of the accessory optic system [30]. There is evidence the circuits can contribute to target selection and decision making but differ in acuity from the primary visual cortical pathways that mediate perceptual discrimination tasks [31–33].

This study had five objectives. First was to fully characterize the spatiotemporal range of rat vision. Prior work has primarily reported on spatial aspects of contrast sensitivity, while temporal aspects have received scant attention. Second was to assess rat vision over a wide luminance range. Prior work was mostly conducted at a single photopic light level. Scotopic measurements are needed, especially since the animal is nocturnal. Third was to model the contrast sensitivity function of rats. Prior work has provided empirical estimates of peak contrast sensitivity and spatial resolution limit, which are informative quantities but

insufficient to quantitatively describe the visibility of any given stimulus to the animal. Fourth was to investigate Brown-Norway rats. This strain is frequently used in glaucoma research, and its visual abilities may differ from those of the more documented Long-Evans and albino strains. In addition, we have long studied the electrophysiological properties of retinal ganglion cells in this strain [34–36], which allows for functional comparisons with their spatiotemporal response characteristics. And fifth was to evaluate the spatial and temporal acuity of the primary and accessory visual systems via task- and reflex-driven behaviors.

Experimental Procedures

Animal preparation

Experiments were carried out in accordance with the recommendations of NIH Guide for the Care and Use of Laboratory Animals and with approval from the USF Institutional Animal Care and Use Committee. Male retired-breeder Brown-Norway rats (300–400g, >6 months old) were purchased commercially (Envigo Inc., Indianapolis, IN) and individually housed under a 12-hour light/12-hour dark cycle in a temperature-controlled room (21°C). Animals had *ad libitum* access to water and restricted access to food to motivate learning and behavior. All experiments were performed during the subjective day (6AM – 6PM), with animal training sessions in the morning and testing sessions in the afternoon.

Visual psychophysics

Figure 1A illustrates the rat visual psychophysics setup, which is a variation of the jump test. Animals were placed inside an acrylic box (50 cm × 40 cm × 46 cm) on a narrow (15 cm × 40 cm) ledge in front of two platforms (20 cm × 20 cm) separated by a vertical divider (width: 1 cm). The ledge and landing platforms were elevated 15 cm to discourage animals from exploring the box and separated by a 6-cm gap so that animals could only reach the platforms by jumping. All surfaces were opaque except for the wall behind the platforms, which was transparent. A CRT monitor (36 cm × 27 cm, 120 Hz non-interlaced) abutted the transparent wall and displayed a solid gray image or a vertical sinewave grating pattern of the same mean gray-level (L) behind each platform. The monitor (Dragonflat D99, Sceptre Inc, Industry, CA) was calibrated with a photometer (UDT Instruments, Baltimore, MD) to give linear output for gratings from 0.01 to 1 in Michelsen contrast ($[L_{max} - L_{min}]/[L_{max} + L_{min}]$). Mean display luminance was 37 cd/m^2, which lies in the photopic range of rat [37]. On the sound of a beep, which indicated the start of a trial, animals had 20 s to jump from the ledge onto one of the landing platforms. They received a food reward (rat chow or honey-nut oat cereal by hand) for crossing to the platform that corresponded to the grating pattern before trial end, which was announced by a noise chirp. Animals naturally adopted the forward-leaning center position illustrated in the figure, translating to a viewing distance of 25 cm. At this distance each half of the screen spanned a 48° × 36° region of visual space. Animals were manually returned to the ledge after each trial, and the side of grating presentation was randomized across trials.

Rats required training to perform the visual task. The training process began by measuring *ad libitum* body weight and daily food intake (DFI) over a one-week period. Thereafter

animals received 80–90% of their average DFI as food rewards during daily training or testing sessions, with any remainder of the DFI allotment deposited in their cages afterward. *Ad libitum* access to food was restored if body weight dipped below 85% of its initial value. The ledge was placed next to the landing platforms at the start of training so that there was no gap to inhibit animal crossings and desired behaviors were guided by hand and liberally rewarded. Gap distance and reward criteria were gradually increased across training sessions until animals performed the task on their own with 90% accuracy for a maximum contrast drifting grating and gap. Figure 1B plots the learning curve of one animal, which exceeded the 90% performance criterion after 18 days.

The visual task presented a two-alternative unforced choice with three possible outcomes on each trial. Animals could either: go to the correct platform, go to the incorrect platform, or do nothing. Contrast detection thresholds were determined from the behavioral decisions of trained animals using an adaptive 1-up-2-down staircase paradigm. The paradigm started with grating contrast of 1 and decreased contrast by 50% after every two correct responses in a row and increased contrast by 50% after every incorrect response. A decrease-to-increase in contrast was defined as a reversal and the paradigm stopped after 5 reversals. Contrast was unchanged if no platform was selected in the allotted time, and five no-choice trials in a row were treated as an incorrect response since the animal did not successfully perform the visual discrimination for whatever reason. This produced a reversal, which allowed the paradigm to continue or end. The contrast values immediately prior to the reversals were then averaged to estimate threshold for a given stimulus. Figure 1C plots behavioral data of a trained rat for a 0.4-cpd drifting grating. It took 52 trials for the paradigm to estimate contrast threshold for this stimulus, which equates to ~20 minutes.

Contrast thresholds were measured daily under scotopic or photopic illumination conditions for rats. Trained animals were transferred in the morning to a dark room and dark adapted for scotopic measurements at least 3 hours prior to afternoon test sessions. Room lights remained off during testing, while the monitor screen was covered with a bank of neutral density filters (sheets 209, 210, 211, 298, 299, Lee Filters, Burbank, CA) that collectively attenuated mean light output by 2, 4, 6, or 8 log units. Animals came light adapted to room illumination (27 cd/m^2) for photopic measurements. Spatial acuity data were collected for 0.01 to 3 cycles/degree (cpd) drifting gratings, and temporal acuity data were collected for 0.01 to 60 Hz contrast-reversing gratings. Temporal frequency (tf) and spatial frequency (sf) were respectively fixed at 6 Hz and 0.2-cpd to maximize grating visibility based on initial testing. Up to four grating parameters were tested each session at one mean light level.

Optomotor responses

Rat vision was also assessed by evoking optomotor responses (OMRs) with a commercial optomotry system (CerebralMechanics Inc, Medicine Hat, Canada). Animals were placed on a small elevated platform at the center of a closed chamber (39 cm × 39 cm × 32.5 cm) walled on four sides by LCD computer monitors. The monitors (27 cm × 33 cm) displayed a vertical grating pattern of varying sf or tf rotating about a virtual cylindrical drum centered on the animal's head [28]. The grating randomly rotated leftward or rightward on each trial, and contrast was adjusted until a threshold was reached where head-tracking movements

were no longer detected by the experimenter who was blind to rotation direction. Head movements were observed from above with a videocamera mounted atop the chamber, and tracking was defined as a repeated smooth movement and reorientation of the head in a given direction within 5 s of stimulus presentation. Contrast thresholds were measured for gratings of varying sf or tf at the mean luminance of the optomotry system (53 cd/m^2), which was in the photopic range of rats.

Data analysis

Contrast threshold data were numerically inverted to contrast sensitivity, combined for each grating stimulus across all test sessions from a given animal, removed of outliers that deviated more than two-fold from the median, and averaged. Contrast sensitivity data have a non-normal distribution, so they were logarithmically transformed and averaged across animals for purposes of presentation of group data. The resulting contrast sensitivity function (CSF) was regressed against grating sf or tf using a truncated log-parabola equation $S(f)$, given by:

$$S(f) = \begin{cases} S_{peak} \cdot (1 - \alpha_{LF}), f < f_{peak} \text{ and } S(f) < S_{peak} \cdot (1 - \alpha_{LF}) \\ S_{peak} \cdot 10^{-\left(\frac{\log_{10}(f) - \log(f_{peak})}{f_{bw}}\right)^2}, elsewhere \end{cases}$$

This equation was selected because it has been shown to fit the CSFs of human subjects [3840] and its parameters are straightforward to interpret. S_{peak} is the maximum contrast sensitivity, f_{peak} is the frequency at which contrast sensitivity is maximal, f_{bw} is the frequency bandwidth, and α_{LF} is the fractional reduction in peak contrast sensitivity at low frequency. Parameter values were estimated in MATLAB (Mathworks Inc, Natick, MA) using a built-in nonlinear regression algorithm (nlinfit). Regression results were then used to determine the frequency resolution limit f_{limit} given by $S(f_{limit}) = 1$. Figure 1D illustrates the five parameters extracted from CSFs. Parameter distributions were analyzed with SigmaPlot (Systat Inc, San Jose, CA) software for statistical significance a one-way repeated measure ANOVA and Student's t-tests at α-level of 0.05.

Results

Contrast sensitivity data were collected from a total of 7 adult rats via the grating detection task and 8 adult rats via the optomotor reflex. Subsets of the former group were used for light- and dark-adapted spatial and temporal frequency measurements. There was no animal overlap between the two groups. Animals took 23 ± 4 days to learn the visual task. No animal training was needed for OMRs.

Psychophysical measurements of spatial contrast sensitivity

Figures 2A plots the CSF of a light-adapted rat for sf gratings drifting at optimal tf. The CSF exhibits a spatial bandpass characteristic under photopic illumination, which was fit by a truncated log-parabola model to summarize key features of the sf data. S_{peak} averaged 51.5 ± 10.3 across animals (n = 5), meaning that the minimum grating contrast that rats could detect at optimal spatiotemporal frequency is ~2%. f_{peak} was 0.15 ± 0.04 cpd and S_{limit}, which

estimates the highest sf that rats can discriminate, was 1.7 ± 0.3 cpd. The sf range of photopic vision was also fairly narrow as f_{bw} was 0.87 ± 0.10 cpd. The narrow bandwidth can be attributed to a marked drop in contrast sensitivity at low sf. α_{LF} was 81 ± 9%, which amounts to more than a 5-fold reduction in peak sensitivity. Figure 2B plots the average log spatial CSF of light-adapted rats. A log scale is used to normalize contrast sensitivity measurements and communicate CSF variability across experiments.

Figure 3A plots the CSFs of a dark-adapted rat for drifting sf gratings of different mean luminance. Animals performed the visual task at chance level when the display luminance was attenuated by 8 log units (not shown), indicating that they were unable to see the grating. Just above the threshold for vision, which is around 6 log units of attenuation, rat contrast sensitivity is poor and the spatial CSF exhibits a fairly lowpass characteristic. Further increases in display luminance from −4 to 0 log units cause a marked enhancement in contrast sensitivity and a progressive transition of the spatial CSF to the bandpass characteristic observed under photopic illumination. Figure 3B plots the average log spatial CSF of dark-adapted rats from which complete datasets were collected for all mean luminance conditions (n = 3). It can be seen in the group average that the high sf cutoff increased systematically with display luminance as well. Figure 3C summarizes the analysis of log-parabola fits to spatial CSFs of these animals. S_{peak} scaled with mean light level by a factor of ~1.4 per log unit ($F = 60.5$; $p < 0.001$; $R^2 = 0.95$). No significant change in f_{peak} or f_{bw} was detected except the −6 log unit condition ($p < 0.05$ for 0 vs. −6 LU for both parameters) despite the change in sf tuning. The lowpass-to-bandpass transition was best captured by α_{LF}, which roughly doubled over the luminance range tested ($F = 6.4$; $p = 0.03$; $R^2 = 0.71$). A small increase in f_{limit} was also noted in moving from scotopic to photopic display luminance ($F = 5.2$; $p = 0.04$; $R^2 = 0.60$), amounting to 0.06 cpd per log unit.

Psychophysical measurements of temporal contrast sensitivity

Figure 4A plots the CSF of a light-adapted rat for gratings reversing contrast at different tf. The temporal CSF exhibits a weak bandpass characteristic under photopic illumination that was similarly fit by the truncated log-parabola model. S_{peak} averaged 43.0 ± 8.6 across animals (n = 3), which was not significantly different from that measured independently from sf data ($p = 0.30$). f_{peak} was 2.6 ± 0.8 Hz, f_{bw} was 1.5 ± 0.1 Hz, and f_{limit} was 198 ± 33 Hz. This estimate of the highest tf that rats can discriminate is constrained in accuracy by the frame rate of the display monitor, which limited data collection to tf below 60 Hz. α_{LF} was 38 ± 8%, reflecting the small reduction in contrast sensitivity at low tf. Figure 4B plot the average log temporal CSF to summarize tf data from light-adapted rats.

Figure 5A plots the CSFs of a dark-adapted rat for reversing tf gratings of different mean luminance. The temporal CSF exhibits a relatively lowpass characteristic at 6 log units of attenuation and progressive transitions a more bandpass characteristic as display luminance is increased. Figure 5B plots the average log temporal CSF of dark-adapted rats from which complete datasets were collected for all mean luminance conditions (n = 4). It can be seen in the group average that the high tf cutoff increased systematically with display luminance, while the slope of the high tf rolloff was fairly constant. This differs from the high sf rolloff of the spatial CSF, which increased in slope with luminance. Figure 5C summarizes the

analysis of log-parabola fits to CSFs of these animals. S_{peak} scaled by a factor of ~1.4 per log unit, as might be expected from the spatial CSF data ($F = 30.4$; $p < 0.001$; $R^2 = 0.74$). In fact, the S_{peak} of the temporal CSF was indistinguishable from the S_{peak} of the spatial CSF at each mean light level (0 LU: $p = 0.41$; −2 LU: $p = 0.05$; −4 LU: $p = 0.30$; −6 LU: $p = 0.41$) though those data were collected from different animals. No significant change in f_{peak} ($F = 3.8$; $p = 0.05$; $R^2 = 0.02$) or f_{bw} ($F = 4.3$; $p = 0.38$; $R^2 = 0.01$) was detected; whereas, f_{limit} scaled with light level by the same factor as S_{peak} of ~1.4 per log unit ($F = 19.7$; $p < 0.001$; $R^2 = 0.66$). The lowpass-to-bandpass transition was again captured by α_{LF}, which approximately doubled for the luminance range tested ($F = 9.2$; $p < 0.01$; $R^2 = 0.58$).

Optomotor measurements of contrast sensitivity

Figures 6A and 6B respectively plot the spatial CSF of a light-adapted rat and log-average spatial CSF of a group of rats (n = 7) as measured via the OMR. It can be seen that the CSF exhibits a spatial bandpass characteristic under photopic illumination but contrast sensitivity and high sf cutoff are much reduced from that measured via the grating detection task. Fits of the truncated log-parabola model yield S_{peak} of 6.1 ± 1.1, f_{peak} of 0.13 ± 0.02 cpd, f_{bw} of 0.59 ± 0.13 cpd, f_{limit} of 0.42 ± 0.07 cpd, and α_{LF} of 71 ± 8%. The reductions in S_{peak}, f_{bw}, and f_{limit} were statistically significant ($p < 0.05$ for all). Figures 6C and 6D respectively plot the temporal CSF of a light-adapted rat and log-average temporal CSF of a group of rats (n = 8) as measured via the OMR. The CSF exhibits a more temporal bandpass characteristic than that measured via the grating detection task, with contrast sensitivity and high tf cutoff again much reduced. Fits of the truncated log-parabola model yield S_{peak} of 6.6 ± 0.9, f_{peak} of 1.9 ± 0.3 Hz, f_{bw} of 0.8 ± 0.1 Hz, f_{limit} of 10 ± 1 Hz, and α_{LF} of 45 ± 27%. The reductions in S_{peak}, f_{bw}, and f_{limit} were statistically significant ($p < 0.05$ for all). CSFs were not measured at different luminance levels from dark-adapted rats, as done with the grating detection task, because the photopic contrast sensitivity of OMRs was too low.

Discussion

This study used a modified version of the visual jump test to quantitatively characterize the spatiotemporal frequency range of vision of Brown-Norway rats from scotopic to photopic light level. The luminance dependence of rat vision is qualitatively similar to that of humans and other higher mammals [41–43]; in that, spatial and temporal CSFs exhibit a bandpass characteristic at high mean luminance and transition to a lowpass characteristic at low mean luminance. The changes in CSF shape are accompanied by analogous decreases in contrast sensitivity, spatial acuity, and temporal acuity. Spatial CSFs were thus well fit by a truncated log-parabola model used to describe spatial contrast detection by humans [38–40]. The model was found to equally fit temporal CSFs of rats. Model results indicate the decreases in contrast sensitivity and spatiotemporal acuity scale roughly linearly with log light attenuation. CSFs were also measured using OMRs, which do not require learning or cognitive processing. Contrast sensitivity and spatiotemporal acuity were several-fold less for this visually-evoked behavior.

Relation to prior behavioral work on rats

The ability of rats to detect spatial grating patterns has been investigated by several groups. None examined temporal grating detection. Most of these studies described spatial vision solely in terms of the highest spatial frequency that animals could resolve, which is consistently around 0.5 cpd for albino rats and 1 cpd for pigmented rats under photopic illumination [12, 17–19, 22, 29, 44, 45]. One study noted that the Fisher-Norway strain had markedly higher spatial acuity of ~1.6 cpd, although Fisher-344 rats are albino, and suggested it may have been inherited from crossing with Brown-Norway rats [22]. Our results confirm the Brown-Norway strain has superior spatial acuity. A few studies provided a more complete description of spatial vision by including CSFs, and the published data were fit by the truncated log-parabola model. Table 1 summarizes model fits to CSF measurements from different rat strains. In addition to better acuity, Brown-Norway rats have greater contrast sensitivity than Long-Evans and albino rats. Other aspects of spatial vision like peak frequency and low frequency attenuation are comparable.

Vision assessment via OMRs underestimates the ability of rats to see. This was noted by a previous study and attributed to the involvement of purely subcortical circuits in eye- and headt-racking behaviors [29]. A common finding with Long-Evans rats has been that OMR spatial acuity is down around 0.5 cpd [29, 46–48]. This was also the case for Brown-Norway rats. There are no reports on the temporal acuity of rat OMRs but it was markedly less as well, averaging 10 Hz compared to over 100 Hz for the grating detection task. The tf limit of OMRs could reflect motor limitations of the head-tracking system [49], but spatial and temporal CSFs both match closely in peak, bandwidth, and cutoff frequency those of superior colliculus neurons [50]. In addition to lower acuity, OMRs of Brown-Norway rats had poor sensitivity. The contrast of an optimal sf and tf grating had to exceed 10 to 15% for the observer to detect head-tracking movements. This is much greater than the contrast thresholds of 1.5 to 3% reported for Long-Evans rats [29, 51, 52]. It is also greater than the 5% typically reported for mice [29, 53–55]. The poor contrast sensitivity cannot be attributed to observer bias because thresholds were consistent across animals even though the data were collected by multiple naïve and blinded observers. It is presumably related to rat strain or their retired-breeder age.

Relation to neural measures of rat contrast sensitivity

The grating detection experiment was designed to facilitate comparison of psychophysical CSFs with neurophysiological CSFs recorded in the lab from optic nerve fibers *in vivo* [34–36]. Aside from the rat being anesthetized, the animal model and stimulus presentation are the same and an algorithm systematically modifies contrast to find the threshold for evoking a criterion modulation of spike firing rate. The inverse of this threshold, referred to as neural responsivity, averages 120 and 200 spikes/sec/unit-contrast at optimal photopic spatiotemporal frequency for X- and Y-like rat ganglion cells, respectively [36]. Spike discharge noise is expected to limit the smallest detectable signal to a modulated rate around 4 spikes/sec [34, 36], so cell responsivity suggests a peak contrast sensitivity of ~50 for Brown-Norway rats. The suggestion is in line with psychophysical measurements though it neglects multicellular processes like cortical integration that might be expected to boost signal-to-noise ratio and raise contrast sensitivity further. Visual acuity, on the other hand, is

poorly predicted by the receptive field properties of X- and Y-like cells. The highest sf and tf that the cells can communicate is around 0.33 cpd [36] and 26 Hz [56], both of which are well below what the animal can resolve.

There are several possible explanations for the marked disparity in neural and perceptual acuity. One is that rats may use edge effects to accomplish the detection task when the grating itself is not visible since display edges can produce a flicker percept in humans [57]. Another is that the rat visual system may construct a higher resolution image from the coincident activity of a mosaic of ganglion cells with overlapping receptive fields [58]. Most likely is that there exists a population of high acuity cells in rats which optic nerve electrodes cannot access. More than 25 functional types of ganglion cell have been identified in the mouse retina using *in vitro* recording techniques [59]. X- and Y-like cells appear to belong to the same morphological class known as alpha ganglion cell given their center-surround organization and similar receptive field sizes [36, 60] and evidence of both sustained and transient varieties of alpha cell in mice [61], and alpha cells have larger receptive fields than other cell types in mice [62, 63] and other mammals [64]. Consistent with the idea some cells in rat visual cortex can respond out to 1.2 cpd in sf and 55 Hz in tf [65].

The spatiotemporal acuity of X- and Y-like cells align well, on the other hand, with that of the OMR. OMR circuitry relies on different retinal output pathways than the primary one through the lateral geniculate nucleus since visual cortical lesions have no effect on rodent head tracking [29, 66]. In further support of this idea, rats with lateral geniculate lesions were unable to detect gratings above 0.7 cpd [67], which approximates the sf limit of OMRs, and cortical inactivation impaired mouse performance on a forced-choice task involving grating detection [68]. Moreover, the superior colliculus is a major target of retinal projections in the accessory optic pathway [30] and neurons in the rat superior colliculus also respond best to sf around 0.02 cpd with a sf limit of 0.4–0.8 cpd [50]. X- and Y-like cells thereby appear to serve subcortical circuits that mediate image stabilization via eye and head movements.

Study limitations

An important limitation to the interpretation of visual behavior studies is animal movements. Grating sf depends on the viewing distance at the unknown time and location of rat detection. While it was well prescribed by the jumping and landing platform design, the head was not in the same spot on every trial for the entire trial duration. The distance that animals leaned forward is estimated to vary up to 1.5 cm from the standard position, which would impart a 5% error of sf values. The perceived TF of drifting gratings is also altered by eye, head, or body rotation. Rats could thereby have improved detection of a non-optimal sf by aliasing the grating to a tf that is more visible to the animal. This may have impacted the shape of spatial CSFs but was mitigated for temporal CSFs by the use of contrast-reversing gratings. Another limitation is the frame rate of the display, which was insufficient to probe very high tf. Temporal acuity estimates involved considerable model extrapolation and are thereby least reliable of reported parameters. There is no assessment method that can completely eliminate these limitations and other technical or interpretational considerations

may arise in altering or restricting movements [15]. The approach used here represents a compromise since the rat's self-selection of a standard viewpoint approximates the positional certainty of methods that constrain the head with a nose cone or affix the head to a rigid apparatus while offering the more natural and easily trainable behavior of methods like the visual water test.

Acknowledgements

This work was supported by the National Institutes of Health R01 EY027037. Authors thank Noredden Bitar, Jordan Carbono, Samantha Chanthalima, Minh Dang, Miral Gomaa, Maria Paula Marchi, Erik Markham, Samuel Morris, Ashita Mukalel, Martin Recalde, Pretti Singh, Chukwubuikem Ume-Ugwa, Yubei Wu, and Carolyna Yamamoto for assistance with perceptual data collection and Krystian Gonzalez and Jacob Yarinsky with OMR data collection.

Abbreviations

CSF	contrast sensitivity function
sf	spatial frequency
tf	temporal frequency
DFI	daily food intake
cpd	cycles per degree
OMR	optomotor response

References

1. Baker M (2013) Neuroscience: Through the eyes of a mouse. Nature 502 (7470), 156–8. [PubMed: 24108031]
2. Leinonen H and Tanila H (2018) Vision in laboratory rodents-Tools to measure it and implications for behavioral research. Behav Brain Res 352, 172–182. [PubMed: 28760697]
3. Reinagel P (2015) Using rats for vision research. Neuroscience 296, 75–9. [PubMed: 25542420]
4. Abbott A (2010) Neuroscience: The rat pack. Nature 465 (7296), 282–3. [PubMed: 20485409]
5. Zoccolan D (2015) Invariant visual object recognition and shape processing in rats. Behav Brain Res 285, 10–33. [PubMed: 25561421]
6. Crawford LE et al. (2020) Enriched environment exposure accelerates rodent driving skills. Behav Brain Res 378, 112309. [PubMed: 31629004]
7. Horner AE et al. (2013) The touchscreen operant platform for testing learning and memory in rats and mice. Nat Protoc 8 (10), 1961–84. [PubMed: 24051959]
8. Oomen CA et al. (2013) The touchscreen operant platform for testing working memory and pattern separation in rats and mice. Nat Protoc 8 (10), 2006–21. [PubMed: 24051961]
9. Aoki R et al. (2017) An automated platform for high-throughput mouse behavior and physiology with voluntary head-fixation. Nat Commun 8 (1), 1196. [PubMed: 29084948]
10. Yu Y et al. (2018) Mice use robust and common strategies to discriminate natural scenes. Sci Rep 8 (1), 1379. [PubMed: 29358739]
11. Whishaw IQ (1995) A comparison of rats and mice in a swimming pool place task and matching to place task: some surprising differences. Physiol Behav 58 (4), 687–93. [PubMed: 8559777]
12. Prusky GT et al. (2000) Behavioral assessment of visual acuity in mice and rats. Vision Res 40 (16), 2201–9. [PubMed: 10878281]

13. Douglas RM et al. (2006) Perception of visual motion coherence by rats and mice. Vision Res 46 (18), 2842–7. [PubMed: 16647739]
14. Cressant A et al. (2007) Spatial learning in Long-Evans Hooded rats and C57BL/6J mice: different strategies for different performance. Behav Brain Res 177 (1), 22–9. [PubMed: 17157932]
15. Zoccolan D and Di Filippo A (2018) Methodological Approaches to the Behavioural Investigation of Visual Perception in Rodents In Handbook of Behavioral Neuroscience (Ennaceur A and Angelica de Souza Silva M eds), pp. 69–101, Elsevier.
16. Lashley KS, The mechanism of vision. I: A method for the rapid analysis of pattern vision in the rat., Journal of Genetic Psychology, 1930, pp. 453–460.
17. Birch D and Jacobs GH (1979) Spatial contrast sensitivity in albino and pigmented rats. Vision Res 19 (8), 933–7. [PubMed: 516464]
18. Legg CR (1984) Contrast sensitivity at low spatial frequencies in the hooded rat. Vision Res 24 (2), 159–61. [PubMed: 6710877]
19. Keller J et al. (2000) Assessing spatial vision - automated measurement of the contrast-sensitivity function in the hooded rat. J Neurosci Methods 97 (2), 103–10. [PubMed: 10788664]
20. Bussey TJ et al. (2008) The touchscreen cognitive testing method for rodents: how to get the best out of your rat. Learn Mem 15 (7), 516–23. [PubMed: 18612068]
21. Morton AJ et al. (2006) Measuring cognitive deficits in disabled mice using an automated interactive touchscreen system. Nat Methods 3 (10), 767. [PubMed: 16990806]
22. Prusky GT et al. (2002) Variation in visual acuity within pigmented, and between pigmented and albino rat strains. Behav Brain Res 136 (2), 339–48. [PubMed: 12429395]
23. Seymoure P and Juraska JM (1997) Vernier and grating acuity in adult hooded rats: the influence of sex. Behav Neurosci 111 (4), 792–800. [PubMed: 9267656]
24. Zoccolan D et al. (2009) A rodent model for the study of invariant visual object recognition. Proc Natl Acad Sci U S A 106 (21), 8748–53. [PubMed: 19429704]
25. Meier PM and Reinagel P (2013) Rats and humans differ in processing collinear visual features. Front Neural Circuits 7, 197. [PubMed: 24379758]
26. Simpson EL and Gaffan EA (1999) Scene and object vision in rats. Q J Exp Psychol B 52 (1), 1–29. [PubMed: 10189831]
27. Kurylo DD et al. (1997) Characteristics of perceptual grouping in rats. J Comp Psychol 111 (2), 126–34. [PubMed: 9170277]
28. Prusky GT et al. (2004) Rapid quantification of adult and developing mouse spatial vision using a virtual optomotor system. Invest Ophthalmol Vis Sci 45 (12), 4611–6. [PubMed: 15557474]
29. Douglas RM et al. (2005) Independent visual threshold measurements in the two eyes of freely moving rats and mice using a virtual-reality optokinetic system. Vis Neurosci 22 (5), 677–84. [PubMed: 16332278]
30. Simpson JI (1984) The accessory optic system. Annu Rev Neurosci 7, 13–41. [PubMed: 6370078]
31. Li X et al. (2015) Comparison of visual receptive field properties of the superior colliculus and primary visual cortex in rats. Brain Res Bull 117, 69–80. [PubMed: 26222378]
32. Crapse TB et al. (2018) A Role for the Superior Colliculus in Decision Criteria. Neuron 97 (1), 181–194.e6. [PubMed: 29301100]
33. Wolf AB et al. (2015) An integrative role for the superior colliculus in selecting targets for movements. J Neurophysiol 114 (4), 2118–31. [PubMed: 26203103]
34. Freeman DK et al. (2008) The maintained discharge of rat retinal ganglion cells. Vis Neurosci 25 (4), 535–48. [PubMed: 18634718]
35. Freeman DK et al. (2010) Retinal ganglion cell adaptation to small luminance fluctuations. J Neurophysiol 104 (2), 704–12. [PubMed: 20538771]
36. Heine WF and Passaglia CL (2011) Spatial receptive field properties of rat retinal ganglion cells. Vis Neurosci 28 (5), 403–17. [PubMed: 21944166]
37. Dodt E and Echte K (1961) Dark and light adaptation in pigmented and white rat as measured by electroretinogram threshold. J Neurophysiol 24, 427–45. [PubMed: 13723365]
38. Watson AB and Ahumada AJ (2005) A standard model for foveal detection of spatial contrast. J Vis 5 (9), 717–40. [PubMed: 16356081]

39. Thurman SM et al. (2016) Predicting individual contrast sensitivity functions from acuity and letter contrast sensitivity measurements. J Vis 16 (15), 15.
40. Zheng H et al. (2018) Measuring the Contrast Sensitivity Function Using the qCSF Method With 10 Digits. Transl Vis Sci Technol 7 (6), 9.
41. Pasternak T and Merigan WH (1981) The luminance dependence of spatial vision in the cat. Vision Res 21 (9), 1333–9. [PubMed: 7314518]
42. De Valois RL et al. (1974) Psychophysical studies of monkey vision. 3. Spatial luminance contrast sensitivity tests of macaque and human observers. Vision Res 14 (1), 75–81. [PubMed: 4204839]
43. Smith RA (1973) Luminance-dependent changes in mesopic visual contrast sensitivity. J Physiol 230 (1), 115–35. [PubMed: 4702414]
44. McGill TJ et al. (2004) Quantification of spatial vision in the Royal College of Surgeons rat. Invest Ophthalmol Vis Sci 45 (3), 932–6. [PubMed: 14985313]
45. Crijns E and Op de Beeck H (2019) The Visual Acuity of Rats in Touchscreen Setups. Vision (Basel) 4 (1).
46. Segura F et al. (2018) Development of optokinetic tracking software for objective evaluation of visual function in rodents. Sci Rep 8 (1), 10009. [PubMed: 29968791]
47. McGill TJ et al. (2007) Intraocular CNTF reduces vision in normal rats in a dose-dependent manner. Invest Ophthalmol Vis Sci 48 (12), 5756–66. [PubMed: 18055829]
48. McGill TJ et al. (2012) Discordant anatomical, electrophysiological, and visual behavioral profiles of retinal degeneration in rat models of retinal degenerative disease. Invest Ophthalmol Vis Sci 53 (10), 6232–44. [PubMed: 22899760]
49. Kretschmer F et al. (2017) Comparison of optomotor and optokinetic reflexes in mice. J Neurophysiol 118 (1), 300–316. [PubMed: 28424291]
50. Prévost F et al. (2007) Spatio-temporal receptive field properties of cells in the rat superior colliculus. Brain Res 1142, 80–91. [PubMed: 17303094]
51. Segura F et al. (2015) Assessment of Visual and Chromatic Functions in a Rodent Model of Retinal Degeneration. Invest Ophthalmol Vis Sci 56 (11), 6275–83. [PubMed: 26431481]
52. Cuenca N et al. (2014) Correlation between SD-OCT, immunocytochemistry and functional findings in an animal model of retinal degeneration. Front Neuroanat 8, 151. [PubMed: 25565976]
53. Guzik-Kornacka A et al. (2016) Nogo-A deletion increases the plasticity of the optokinetic response and changes retinal projection organization in the adult mouse visual system. Brain Struct Funct 221 (1), 317–29. [PubMed: 25284126]
54. Grillo SL et al. (2018) Quantification of Changes in Visual Function During Disease Development in a Mouse Model of Pigmentary Glaucoma. J Glaucoma 27 (9), 828–841. [PubMed: 30001268]
55. Prusky GT et al. (2006) Enhancement of vision by monocular deprivation in adult mice. J Neurosci 26 (45), 11554–61. [PubMed: 17093076]
56. Johnson N et al. (2019) Temporal properties of the receptive field center of rat retinal ganglion cells in vivo. Invest Ophthalmol Vis Sci 60, 5282.
57. Campbell FW et al. (1969) Visibility of aperiodic patterns compared with that of sinusoidal gratings. J Physiol 204 (2), 283–98. [PubMed: 5824639]
58. Meister M (1996) Multineuronal codes in retinal signaling. Proc Natl Acad Sci U S A 93 (2), 609–14. [PubMed: 8570603]
59. Sanes JR and Masland RH (2015) The types of retinal ganglion cells: current status and implications for neuronal classification. Annu Rev Neurosci 38, 221–46. [PubMed: 25897874]
60. Stone C and Pinto LH (1993) Response properties of ganglion cells in the isolated mouse retina. Vis Neurosci 10 (1), 31–9. [PubMed: 8424927]
61. Pang JJ et al. (2003) Light-evoked excitatory and inhibitory synaptic inputs to ON and OFF alpha ganglion cells in the mouse retina. J Neurosci 23 (14), 6063–73. [PubMed: 12853425]
62. Zhang Y et al. (2012) The most numerous ganglion cell type of the mouse retina is a selective feature detector. Proc Natl Acad Sci U S A 109 (36), E2391–8. [PubMed: 22891316]
63. Jacoby J and Schwartz GW (2017) Three Small-Receptive-Field Ganglion Cells in the Mouse Retina Are Distinctly Tuned to Size, Speed, and Object Motion. J Neurosci 37 (3), 610–625. [PubMed: 28100743]

64. Troy JB and Shou T (2002) The receptive fields of cat retinal ganglion cells in physiological and pathological states: where we are after half a century of research. Prog Retin Eye Res 21 (3), 263–302. [PubMed: 12052385]

65. Girman SV et al. (1999) Receptive field properties of single neurons in rat primary visual cortex. J Neurophysiol 82 (1), 301–11. [PubMed: 10400959]

66. Harvey RJ et al. (1997) The early phase of horizontal optokinetic responses in the pigmented rat and the effects of lesions of the visual cortex. Vision Res 37 (12), 1615–25. [PubMed: 9231228]

67. Dean P (1981) Visual pathways and acuity hooded rats. Behav Brain Res 3 (2), 239–71. [PubMed: 7271990]

68. Treviño M et al. (2018) An Automated Water Task to Test Visual Discrimination Performance, Adaptive Strategies and Stereotyped Choices in Freely Moving Mice. Front Behav Neurosci 12, 251. [PubMed: 30467467]

Highlights

- Luminance dependence of rat vision is qualitatively similar to that of other mammals
- Rat contrast sensitivity functions were well fit by a truncated log-parabola model
- Acuity and contrast sensitivity of Brown-Norway rats is greater than other rat strains
- Optomotor responses underestimate the visual ability of rats
- Perceptual acuity is comparable to neural acuity of rat visual cortical cells

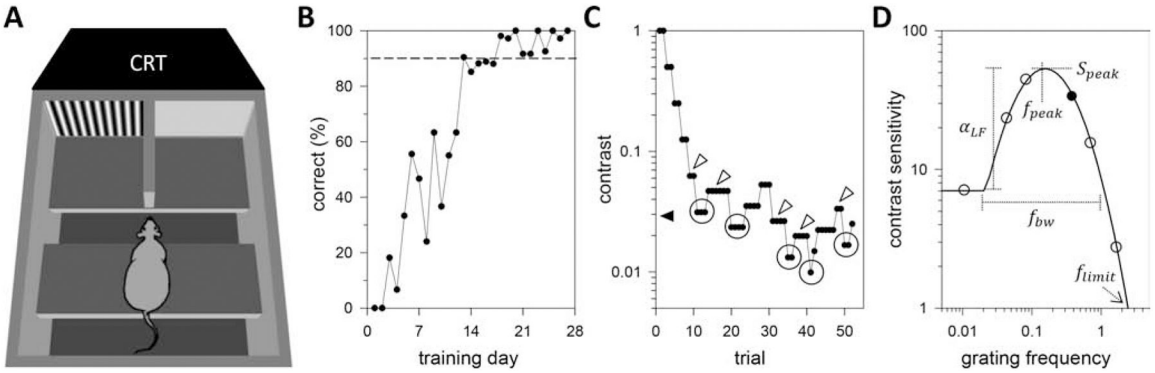

Figure 1.

Assessing rat vision. (A) Animals were trained to jump from a narrow ledge onto the one of two landing platforms behind which a vertical sinewave grating pattern was displayed in order to receive a food reward. The grating drifted at optimal temporal frequency for spatial acuity measurements and reversed contrast at optimal spatial frequency for temporal acuity measurements. Animals naturally adopted the position of facing a thin partition that bisected the screen and separated the two landing platforms, which fixed viewing distance. (B) Percentage of trials that a naïve rat correctly identified a maximum-contrast grating across training sessions. Vision testing began when correct performance exceeded 90% (dashed line). (C) Contrast threshold data of a trained animal across trials in a single testing session. Contrast was raised or lowered each trial using an adaptive one-up-two-down staircase method. The method ended after five contrast reversals (circles) and pre-reversal contrast values (white arrowheads) were averaged to estimate threshold for the grating stimulus (black arrowhead). (D) Modeling contrast sensitivity functions. Reversal data were converted to contrast sensitivity via numerical inversion and regressed against grating frequency by a truncated log-parabola model (line), yielding five parameters (S_{peak}, f_{peak}, f_{bw}, f_{limit}, α_{LF}). Filled and unfilled symbols respectively plot contrast sensitivity measurement of panel C and example data for other grating frequencies.

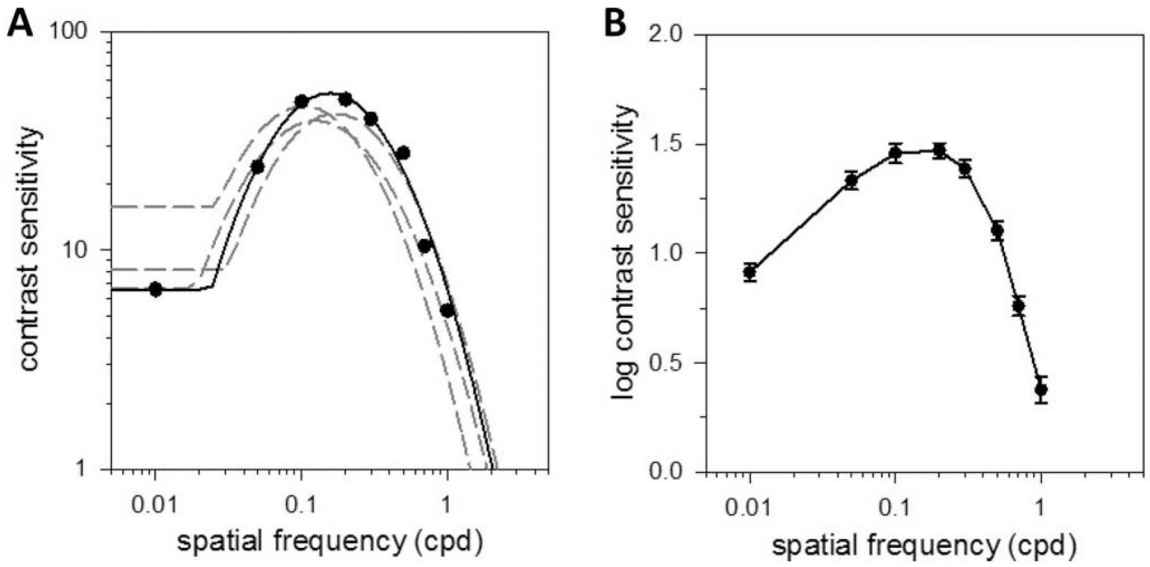

Figure 2.

Spatial vision under photopic illumination. (A) Contrast sensitivity function of a light-adapted rat measured via the grating detection task with sinewave gratings of variable spatial frequency drifting at 6 Hz. Solid line is a fit of a truncated log-parabola model (S_{peak} = 52, f_{peak} = 0.15 cpd, f_{bw} = 0.85 cpd, f_{limit} = 2.05 cpd, α_{LF} = 0.87) to the data. Dashed lines are model fits of all other animals tested. (B) Log-average contrast sensitivity function of 5 light-adapted rats. Error bars are standard error.

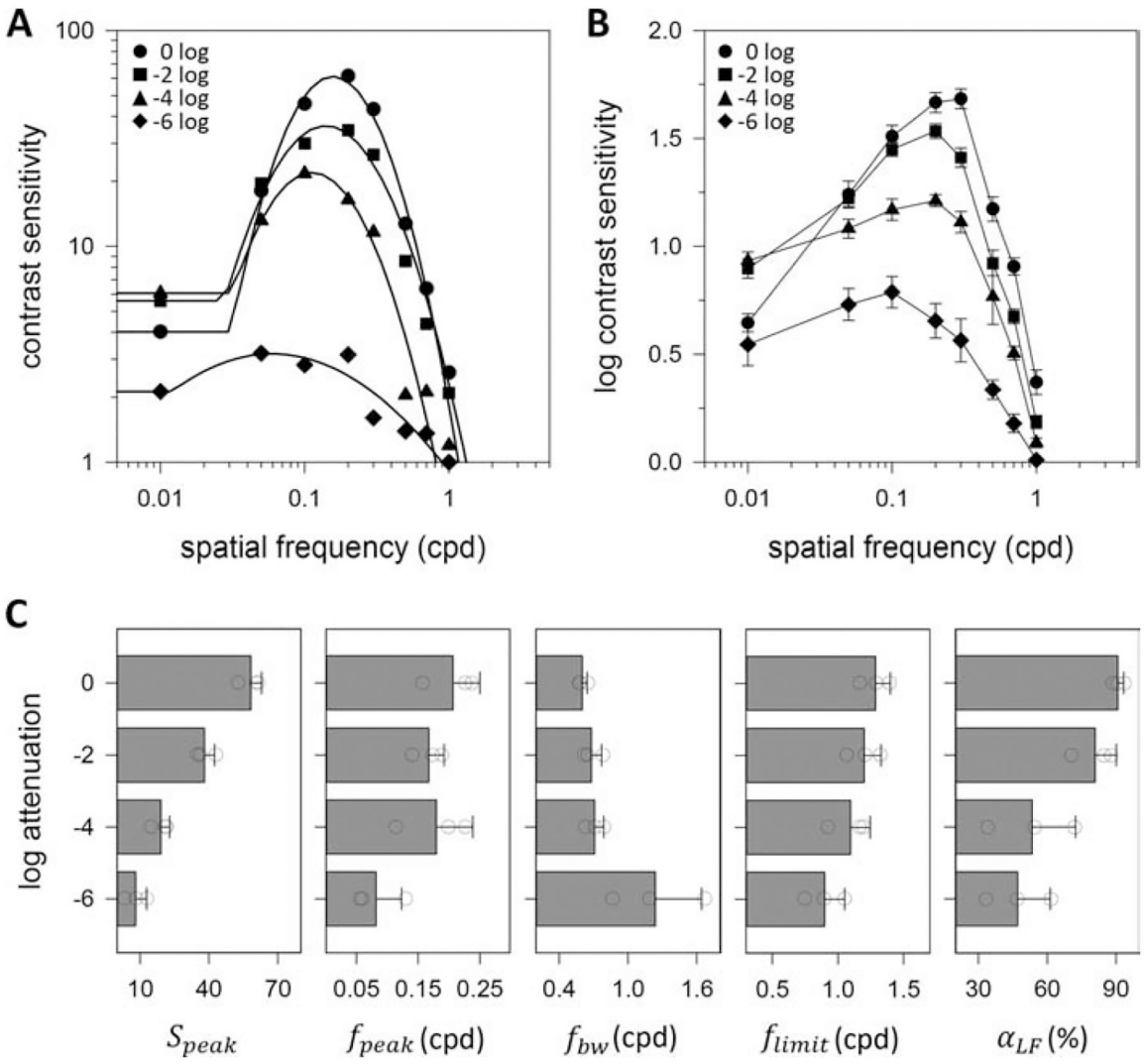

Figure 3.

Spatial vision under varying luminance level. (A) Spatial contrast sensitivity functions of a dark-adapted rat measured via the grating detection task for 6-Hz drifting gratings attenuated in mean luminance by 0 to 6 log units. Solid lines are fits of the truncated log-parabola model to the 0 log (S_{peak} = 61, f_{peak} = 0.16 cpd, f_{bw} = 0.65 cpd, f_{limit} = 1.17 cpd, α_{LF} = 0.93), −2 log (S_{peak} = 36, f_{peak} = 0.14 cpd, f_{bw} = 0.78 cpd, f_{limit} = 1.32 cpd, α_{LF} = 0.85), −4 log (S_{peak} = 21, f_{peak} = 0.11 cpd, f_{bw} = 0.79 cpd, f_{limit} = 0.93 cpd, α_{LF} = 0.72), and −6 log (S_{peak} = 3, f_{peak} = 0.06 cpd, f_{bw} = 1.66 cpd, f_{limit} = 0.89 cpd, α_{LF} = 0.33) data. (B) Log-average contrast sensitivity functions of 3 dark-adapted rats. Error bars are standard error. (C) Average values of model parameters across mean luminance levels for the 3 dark-adapted rats. Error bars are standard deviation. Circles indicate values of individual rats.

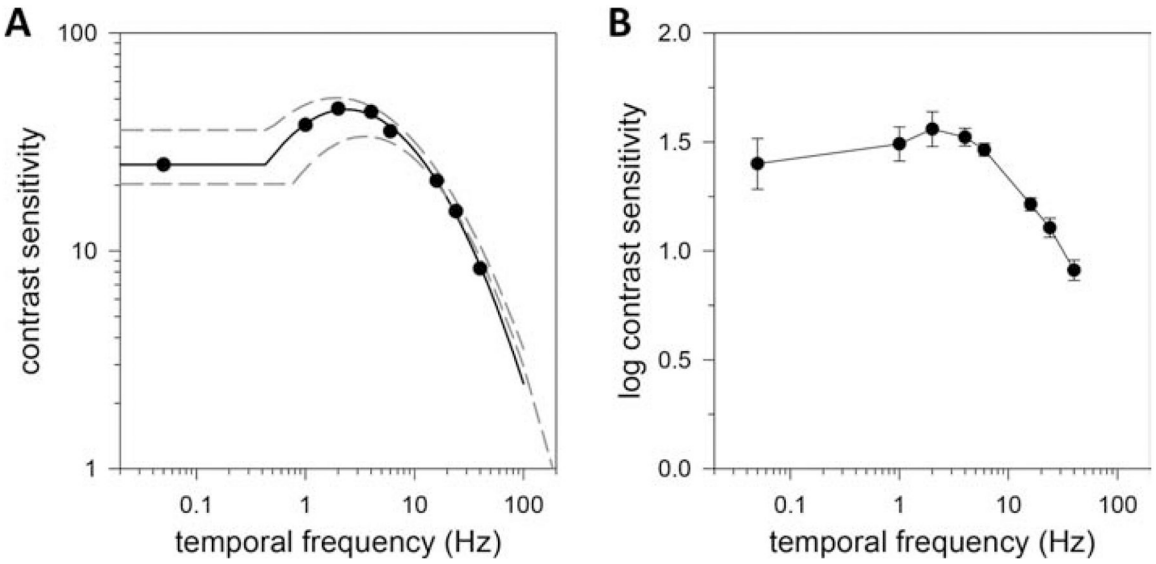

Figure 4.

Temporal vision under photopic illumination. (A) Contrast sensitivity function of a light-adapted rat measured via the grating detection task with 0.2-cpd sinewave gratings reversing contrast at variable frequency. Solid line is a fit of a truncated log-parabola model (S_{peak} = 34, f_{peak} = 3.5 Hz, f_{bw} = 1.4 Hz, f_{limit} = 186 Hz, α_{LF} = 0.41) to the data. Dashed lines are model fits of all other animals tested. (B) Log-average contrast sensitivity function of 3 light-adapted rats. Error bars are standard error.

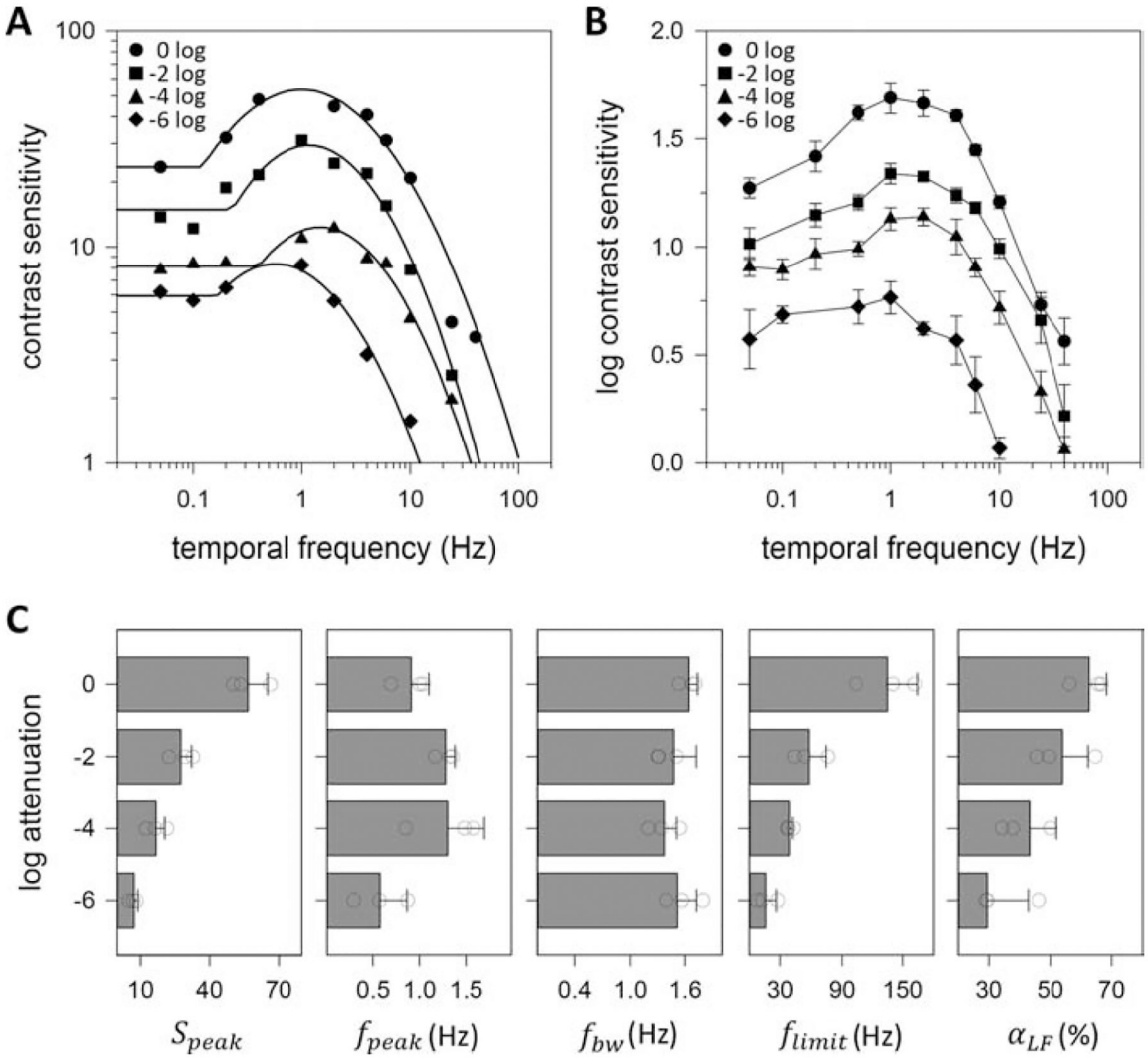

Figure 5.

Temporal vision under varying luminance level. (A) Temporal contrast sensitivity functions of a dark-adapted rat measured via the grating detection task for 0.2-cpd reversing gratings attenuated in mean luminance by 0 to 6 log units. Solid lines are fits of the truncated log-parabola model to the 0 log (S_{peak} = 54, f_{peak} = 1.0 Hz, f_{bw} = 1.5 Hz, f_{limit} = 104 Hz, α_{LF} = 0.56), −2 log (S_{peak} = 30, f_{peak} = 1.2 Hz, f_{bw} = 1.3 Hz, f_{limit} = 44 Hz, α_{LF} = 0.49), −4 log (S_{peak} = 13, f_{peak} = 1.5 Hz, f_{bw} = 1.3 Hz, f_{limit} = 37 Hz, α_{LF} = 0.34), and −6 log (S_{peak} = 8, f_{peak} = 0.6 Hz, f_{bw} = 1.4 Hz, f_{limit} = 12 Hz, α_{LF} = 0.25) data. (B) Log-average contrast sensitivity functions of 4 dark-adapted rats. Error bars are standard error. (C) Average values of model parameters across mean luminance levels for the 4 dark-adapted rats. Error bars are standard deviation. Circles indicate values of individual rats.

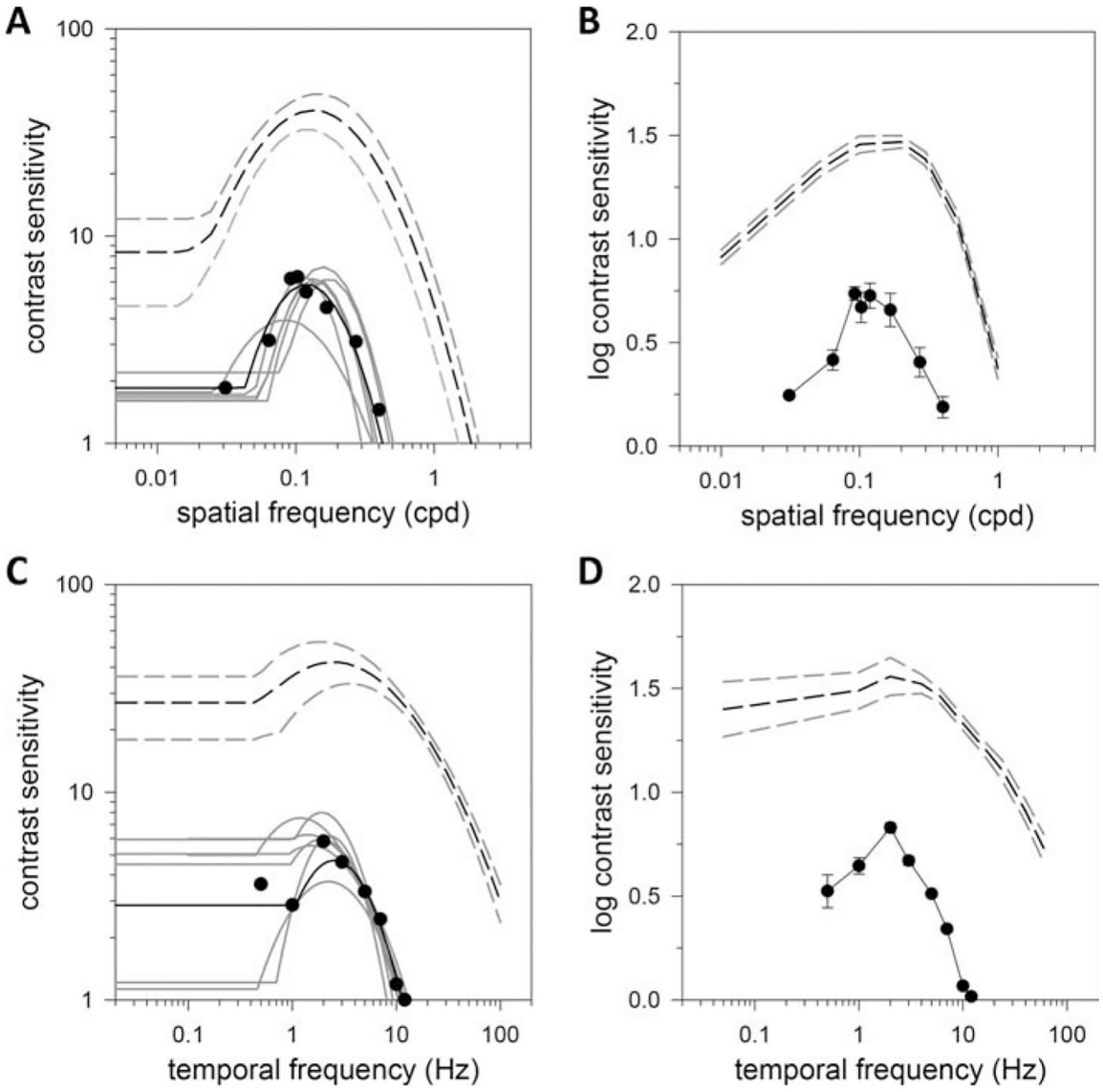

Figure 6.

Comparison of task- and reflex-driven measures of rat vision. (A) Spatial contrast sensitivity function of oculomotor responses of a light-adapted rat for 2-Hz drifting gratings. Solid black line is a fit of a truncated log-parabola model (S_{peak} = 6, f_{peak} = 0.12 cpd, f_{bw} = 0.63 cpd, f_{limit} = 0.43 cpd, α_{LF} = 0.68) to the data. Solid gray lines are model fits of all other animals tested. Black and gray dashed lines plot the fit of the average spatial acuity data in Fig. 2A and the 95% confidence interval, respectively. (B) Log-average spatial contrast sensitivity function of oculomotor responses of 7 light-adapted rats. Error bars are standard error. Black and gray dashed lines plot the log-average spatial acuity data in Fig. 2B and the 95% confidence interval. (C) Temporal contrast sensitivity function of oculomotor responses of a light-adapted rat for 0.2-cpd drifting gratings. Solid black line is a fit of a truncated log-parabola model (S_{peak} = 7, f_{peak} = 1.7 Hz, f_{bw} = 0.9 Hz, f_{limit} = 10.2 Hz, α_{LF} = 0.57) to the data. Solid gray lines are model fits of all other animals tested. Black and gray dashed lines plot the fit of the average temporal acuity data in Fig. 4A and the 95% confidence interval.

(D) Log-average temporal contrast sensitivity function of oculomotor responses of 8 light-adapted rats. Error bars are standard error. Black and gray dashed lines plot the log-average temporal acuity data in Fig. 4B and the 95% confidence interval.

Table 1.

Summary of CSF parameters from grating detection studies performed on different rat strains. Dashes indicate the parameter cannot be estimated because grating frequencies below f_{peak} were not tested. Brown-Norway data of this study were combined for light-adapted and 0-log unit dark-adapted experiments since the display luminance in both cases is 37 cd/m^2.

strain	luminance	S_{peak}	f_{peak}(cpd)	f_{bw} (cpd)	f_{limit} (cpd)	α_{LF} (%)	# rats	
Spatial Contrast Sensitivity								
albino	3.4 cd/m^2	12.4	0.05	1.07	0.6	-	2	[17]
Long Evans	3.4 cd/m^2	20.8	0.13	0.97	1.15	-	2	[17]
	5 cd/m^2	12.6	0.13	0.63	0.60	67	6	[18]
	51 cd/m^2	6.1	0.15	0.78	0.74	75	7	[19]
	36 cd/m^2	36.4	0.20	0.53	0.91	93	4	[28]
	43 cd/m^2	23.7	0.19	0.58	0.92	87	6	[29]
Brown Norway	37 cd/m^2	54.4 ± 8.6	0.17 ± 0.05	0.77 ± 0.16	1.6 ± 0.3	85 ± 9	5	
	37×10^{-2} cd/m^2	38.0 ± 4.4	0.17 ± 0.02	0.68 ± 0.09	1.2 ± 0.1	81 ± 9	3	
	37×10^{-4} cd/m^2	19.1 ± 3.8	0.18 ± 0.06	0.71 ± 0.08	1.1 ± 0.1	53 ± 19	3	
	37×10^{-6} cd/m^2	8.0 ± 4.8	0.08 ± 0.04	1.24 ± 0.40	0.9 ± 0.2	47 ± 14	3	
Temporal Contrast Sensitivity								
Brown Norway	37 cd/m^2	50.3 ± 10.7	1.7 ± 1.1	1.6 ± 0.1	166 ± 44	55 ± 12	5	
	37×10^{-2} cd/m^2	27.5 ± 4.6	1.4 ± 0.3	1.5 ± 0.2	58 ± 17	54 ± 8	4	
	37×10^{-4} cd/m^2	16.8 ± 3.7	1.3 ± 0.4	1.4 ± 0.1	39 ± 4	43 ± 9	4	
	37×10^{-6} cd/m^2	7.2 ± 1.7	0.6 ± 0.3	1.5 ± 0.2	16 ± 10	29 ± 13	4	